Selection of proper combine harvesters to field conditions by an effective field capacity prediction model

Khunnithi Doungpueng[1,2], Khwantri Saengprachatanarug[1,2], Jetsada Posom[1,2], Somchai Chuan-Udom[1,2*]

(1. *Department of Agricultural Engineering, Faculty of Engineering, Khon Kaen University, Khon Kaen 40002, Thailand*; 2. *Applied Engineering for Important Crops of the North East Research Group, Khon Kaen University, Khon Kaen 40002, Thailand*)

Abstract: Farmers have to finish their harvesting with high efficiency, because of time and cost. However, farmers are lacking knowledge and information required for selecting suitable combine harvesters and giving the conditions of their rice fields, because both information factors (combine harvester and field condition) impact the field capacity. The field capacity model was generated from combine harvesters with the Thai Hom Mali rice variety (KDML-105). Therefore, this study aimed to determine the prediction model for effective field capacity to combine harvesters when harvesting the Thai Hom Mali rice variety (KDML-105). The methods began by collecting data of 15 combine harvesters, such as field, crop, and machine conditions and operating times; to generate the prediction model for the KDML-105 variety. The prediction model was then validated using 12 combine harvesters that were collected similarly to the model creation. The results showed a root mean square error (*RMSE*) of 0.24 m^2/s for the model. The prediction model can be applied for farmers to select the proper combine harvesters and give their field conditions.

Keywords: rice harvesting, combine harvester, prediction model, effective field capacity, selection of combine harvester
DOI: 10.25165/j.ijabe.20201304.4984

Citation: Doungpueng K, Saengprachatanarug K, Posom J, Chuan-Udom S. Selection of proper combine harvesters to field conditions by an effective field capacity prediction model. Int J Agric & Biol Eng, 2020; 13(4): 125–134.

1 Introduction

Climate change is an issue that warrants study because it is a problem presently damaging agricultural production. Climate change causes temperature changes, heavy rainstorms, serious drought and severe flooding[1,2], which affect Southeast Asia and particularly countries in the Lower Mekong region such as Cambodia, Laos, Vietnam and Thailand. These countries are heavily impacted by floods during the annual flood season (June-November)[3]. The Mekong River Commission[4] reported that in 2000-2002, annual flooding in these countries resulted in 1380 deaths and a loss of 650 million USD.

In 2011, Thailand produced approximately 34.5 million tons of grain rice, one-third of global rice exports[5]. However, Thailand frequently faces severe floods that negatively affect agricultural activity[6]. Specifically, extreme flooding in Thailand was recorded in 2011, causing a severe disaster that damaged approximately 1.6 million hm^2 of rice production areas (12.5% of the country's cropland) and a loss of 1.3 billion USD[7-9].

The factor to the loss of rice products is a short harvesting season, which is determined by uncontrollable variables like monsoons and natural disasters[10,11]. Farmers have to work under time pressure to finish harvesting before oncoming monsoons and natural disasters. It is thus essential to know the approximate time requirements for finishing a rice harvest. Poor management of harvesting services results in long harvesting times, which is a key problem[12]. Harvesting service providers in Thailand have historically been controlled and managed by local agencies. These agencies are usually operated using only their previous experience. It is routine work and they focus on profits but are not concerned with machine performance.

A large number of Thai farmers do not own combine harvesters but instead, hire from combine providers. In addition, farmers require large combines to harvest in a timely manner when the harvesting season comes[13]. However, most of the combine harvesters lose harvesting times due to turning on headlands, repairs and adjustment times[14] since the use of combine harvesters is not suitable for the field conditions. Moreover, the farmers cannot control the harvesting schedule, since their choices are limited and they have to wait for the providers, which causes a delay in the harvesting time. Nevertheless, Thai farmers are still lacking knowledge, information and technology for selecting suitable combine harvesters matching their rice field conditions. Knowledge of the time and cost consumptions and harvester capacity prior to the harvesting activity is thus essential. This knowledge can be used to select the proper combine harvesters, which help in planning the harvest and estimate the effective field capacity[15]. To the best of our knowledge, there are currently no reports on the development of effective field capacity as a predictive tool for rice fields.

Related topics have been studied by various researchers who developed mathematical models to predict combine harvester

Received data: 2019-02-18 **Accepted data:** 2020-05-09
Biographies: Khunnithi Doungpueng, PhD, research interests: agricultural machinery, Email: khunnithi.d@gmail.com; **Khwantri Saengprachatanarug,** Ph.D., Associated Professor, research interests: agricultural engineering, Email: khwantri@kku.ac.th; **Jetsada Posom,** PhD, Assistant Professor, research interests: biosensor, Email: jetspo@kku.ac.th.
***Corresponding author: Somchai Chuan-Udom,** PhD, Associated Professor, research interests: agricultural mechanization. Department of Agricultural Engineering, Faculty of Engineering, Khon Kaen University, 123 Mittraphap Road, Khon Kaen, 40002, Thailand. Tel: +668-9712-1247, Email: somchai.chuan@gmail.com.

performance. Baruah and Panesar[16,17] predicted the power consumption of Indian combine harvesters for paddy and wheat varieties. Jarolmasjed et al.[18] developed a mathematical model for header loss of the combine harvesters in Iran; the model had a 76% correlation coefficient. Junsiri and Chinsuwan[19] demonstrated the header loss prediction model for combine harvesters in Thailand, with a coefficient of determination (R^2) of 0.75. Chuan-Udom and Chinsuwan[20] developed the threshing loss model of the combine harvester in Thailand; the results satisfied their hypothesis, with a coefficient of determination of 0.92. Sangwijit and Chinsuwan[21] predicted the total loss of combine harvesters and the developed model gave R^2 of 0.91. Liang et al.[22] developed a threshing model and found that combine performance could be improved by analyzing and optimizing the structure and variables of the threshing unit. Siska and Hurburgh[23] developed the corn breakage prediction model using multiple linear regression techniques, with R^2 of 0.65. Additionally, Maertens et al.[24], Maertens and De Baerdemaeker[25] and Miu and Kutzbach[26] forecasted the characteristics of the material moving inside combine harvesters.

Researchers have not only focused on the harvesting loss but they also attended to external factors such as crop and field area[27], the weight of ear[28], crop properties[29,30] and weather conditions[31] which all had an effect on combine performance. Moreover, harvesting robots were developed for strawberries[32], cucumbers[33], apples[34,35], sweet-peppers[36], citrus[37], and lychee[38,39]. These studies support the farmers' works and solve problems in an aging population and decrease labor. The robots worked without human decisions and could work quickly with an increase in field capacity.

Therefore, the goal of this study is to develop an effective field capacity model generated from combine harvesters for the KDML-105 variety. The model will provide useful information for the user in planning the proper Combine harvester matching the field conditions. The model benefits the user through shorter harvesting times, achieving production capacity, and reducing the risk of rice production damage. It can also be adapted in the future to an application for smartphones.

2 Assumptions and theories

2.1 Assumptions and scope of work

Field shape can have an effect on the effective field capacity of the combine harvesters[40]. This study assumed that most fields are rectangular because this shape is easy for construction and water management. The combine harvesters were selected in this study because their dimension, size and assembly parts are different from the western combine harvester[41]. This combine harvester is the commercial machines designed and for work in the ASEAN rice field. Thai Hom Mali rice variety (KDML-105) was selected for the experiment because this variety is of high value and quality, favored by Thai farmers for cultivation[42].

2.2 Theory of effective field capacity

There are two kinds of field capacity of the combine harvester, namely the theoretical field capacity (*TFC*) and effective field capacity (*EFC*). The equations of field capacity are shown in Equations (1) and (2), respectively.

$$TFC = \frac{Atotal}{Tth} \quad (1)$$

$$EFC = \frac{Atotal}{Ttotal} \quad (2)$$

where, *TFC* is theoretical field capacity, m^2/s; *EFC* is effective field capacity, m^2/s; *Atotal* is total harvesting area, m^2; *Tth* is theoretical field time, s; *Ttotal* is total harvesting time, s.

The TFC can be found from the combines harvester without any loss times from operating times[43]. However, in practice, there is no combine harvester without loss times because there are several factors in the practical fields that affect combine harvesters' behavior when harvesting such as crop, field and machine. These factors cause loss times and will be combined with *Tth* into *Ttotal*. All operating times are the factors that the combines normally encounter during practical harvesting, which are as following situations:

(1) The daily preparation time in the garage before leaving to harvest.

(2) The transportation time for moving the combine harvester from the garage to the field and back from the field to the garage.

(3) The preparation time in the field, including daily service time and the time before the start and finish of harvesting.

(4) The theoretical time that does not include the non-operating time, which is calculated by multiplying the effective width and traveling speed[44].

(5) The headland or corners turning time of the field that causes the combine harvester to stop[45-47].

(6) The grain unloading time (not including harvesting) due to unloading grain when the combine is full. Combine harvesters have the grain tank on top of the machine and they need to temporarily halt harvesting and move to the waiting truck trailer on the road or bunds[46]. However, this is not necessary for the western combine harvesters that can unload the grains while harvesting.

(7) The repair, adjustment, and refueling time during the harvesting. This includes any accidents that may cause the harvesting to stop.

(8) The combine harvester operator self-time.

Some operating time activities may not cause time loss from harvesting, such as the times in situations (1)-(3), because these activities happen before the combine harvesters begin their harvesting. In addition, the time in the situation (8) may also not result in time loss because it is out of control, unstable, and the combine is still not active. On the other hand, the activities in situations (4)-(7) happen while the combine harvester is working in the field and are called the total lost time (*TL*). This TL is separated into the headlands and corners turning lost time (*Tn*), the traveling for unloading and grain unloading time without harvesting (*Tf*), and the repair, adjustment, and refueling time during the harvesting (*Tm*). In addition, the rice fields are enclosed by bunds, which are used for water and irrigation management[48]. The combine harvester loses time for bunds crossings, which can be called the bunds crossing lost time (*Tb*). Finally, the *EFC* can be obtained from Equation (3).

$$EFC = \frac{Atotal}{Tth + TL} = \frac{Atotal}{Tth + (Tn + Tm + Tf + Tb)} \quad (3)$$

where, *TL* is total lost time, s; *Tn* is headlands and corners turning lost time, s; *Tn* is headlands and corners turning lost time, s; *Tf* is traveling for unloading and grain unloading lost time, s; *Tm* is repair, adjustment, and refueling lost time during the harvesting, s; *Tb* is bund crossing lost time, s.

2.3 Development of the fundamental prediction model

Equation (3) shows the equation for EFC that consists of the total harvesting area (*Atotal*), theoretical field time (*Tth*) and the

four lost times (*Tn*, *Tf*, *Tm* and *Tb*). The developed methods for the prediction model of *Tth*, *Tn*, *Tf*, *Tm* and *Tb* will be shown in this section and are combined as a fundamental prediction model in the final section.

The flowchart in Figure 1 shows the standard harvesting processes when combine harvesters are working in practical rice fields and possible lost times. The *Tn* was calculated by combining the headland turning lost times (*Tnt*) and the corners turning lost times (*Tnc*); these lost times occur when the combines are harvesting. Similarly, the traveling for unloading lost time (*Tfr*) and the grain unloading lost time (*Tfs*) were included in the *Tf*; these occur when the grain tank is full. In addition, the *Tth* happens only when the combines are harvesting. However, there is no *Tm* included in the flowchart, because this lost time will be included when combine harvesters stop for repairs, adjustments, and refueling.

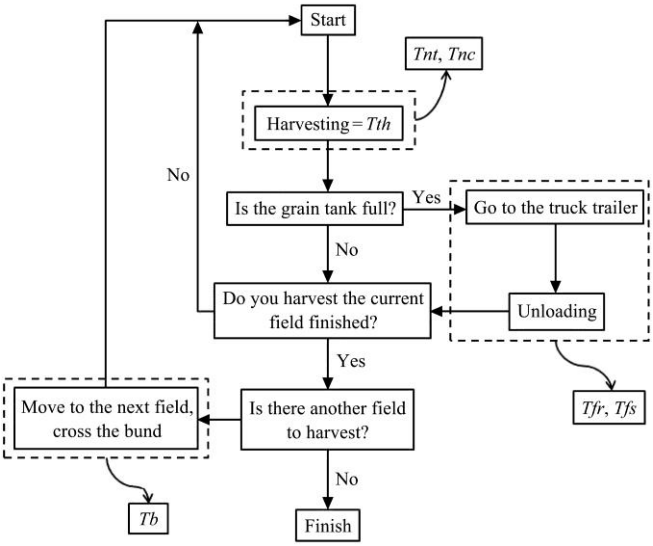

Figure 1 Combine harvesters' harvesting processes in practical fields

2.3.1 Development of the prediction model for the theoretical field time (*Tth*)

If a combine harvester has a header width (*W*) equal to the field width and harvests with a constant traveling speed (*S*), then harvesting is finished without *TL*. The *TFC* and *Tth* can be found from Equations (4) and (5), respectively[44,49]. However, the combine harvesters have to take into account several variables in practical harvestings, such as the physical properties of the crop. This study used the KDML-105 rice variety as a sample, which had a strong effect on the Tth because of its specific physical property of a long stem. This property also affected the header and threshing unit[19,20]. Thus, the coefficient of the theoretical field time (*kth*) was used to adjust the *Tth* for greater accuracy.

$$TFC = W \cdot S = \frac{Atotal}{Tth} \tag{4}$$

$$Tth = \frac{kth \cdot Atotal}{W \cdot S} \tag{5}$$

where, *W* is header width, m; *S* is traveling speed, m/s; *kth* is coefficient of the theoretical field time.

2.3.2 Development of prediction model for the headland and corner turning lost time (*Tn*)

Most farmland in the world has borders and requires farm harvesters to turn at the headland or corners. The combine harvesters encounter a similar process, and lost time due to headland turning and corner turning will occur. Therefore, the development of the prediction model for headland and corner turning lost time will be described in this section.

2.3.2.1 Development of the prediction model for the corner turning lost time (*Tnc*)

The Combine harvester working is shown in Figure 2 with the combine harvesters at the starting point (corner 1, CN1). Following this, the Combine harvester travels and harvests to corner 2 (CN2), but does not immediately make a headland turning due to a risk of damaging unharvested rice. Therefore, the harvester turns left and moves to corner 3 (CN3) and 4 (CN4), respectively. These trips are called "the first-round of harvesting". The first harvested area is shown in Figure 2, but most combine harvesters normally have 2.80-3.20 m of header width. As a result, the first harvested area was insufficient for turning at the headland, and the combine harvesters must have a second round of harvesting. The procedures for the second round are similar to the first. The equations for corner turning in the first and second rounds of harvesting (*T*1 and *T*2, respectively) are shown in Equations (6) and (7), respectively. Furthermore, the *Tnc* is obtained by Equation (8). Finally, the area of the first and second rounds of harvesting (*Ah*1 and *Ah*2, respectively) are shown in Figure 2 and both areas are obtained from Equations (9) and (10), respectively;

$$T1 = T11 + T12 + T13 + T14 = \sum_{i=1}^{4} T1i \quad (6)$$

$$T2 = T21 + T22 + T23 + T24 = \sum_{i=1}^{4} T2i \quad (7)$$

$$Tnc = \sum_{i=1}^{4} T1i + \sum_{i=1}^{4} T2i \quad (8)$$

$$Ah1 = D \cdot W + D \cdot W + b \cdot W + b \cdot W = 2(D \cdot W) + 2(b \cdot W) \quad (9)$$

$$Ah2 = d \cdot W + d \cdot W + bnet \cdot W + bnet \cdot W = 2d \cdot W + 2bnet \cdot W \quad (10)$$

where, *T*11, *T*12, *T*13 and *T*14 are corners turning lost time at the field corner number 1, 2, 3 and 4, respectively in the first round of harvesting, s; $\sum_{i=1}^{4} T1i$ is total corner turning lost time of the first round of harvesting, s; *T*21, *T*22, *T*23 and *T*24 are turning time at the field corner numbers 1, 2, 3 and 4, respectively, in the second round of harvesting, s; $\sum_{i=1}^{4} T2i$ is total corner turning lost time of the second round of harvesting, s; *Tnc* is corner turning lost time, s; *Ah*1 is the area of the first round of harvesting, m^2; *D* is total field length, m; *b* is field width of the area after the first round of harvesting, m; *Ah2* is the area of the second round of harvesting, m^2; *d* is field length after the first round of harvesting, m; *bnet* is net harvesting area width, m.

2.3.2.2 Development of the prediction model for the headland turning lost time (*Tnt*)

Figure 2 shows the field width of the area after the first round of harvesting (*b*), which is the difference between *B* and 2*W* (*b*= *B*–2*W*). Next, the field length after the first round of harvesting (*d*) is the difference between *D* and 2*W* (*d*=*D*–2*W*). The net harvesting area width (*bnet*) is the difference between *B* and 4*W* (*bnet*=*B*–4*W*). Furthermore, *Ah1* and *Ah2* were modified as shown in Equations (11) and (12), respectively. The total area of the first and second rounds of harvesting (*Ah total*) is calculated by the combination of *Ah*1 and *Ah*2, shown in Equation (13). The net harvesting area (*Anet*) is computed by the difference between *Atotal* and *Ah total*, or can be computed by multiplying the net harvesting area width (*bnet*) by the net harvesting area length (*dnet*), shown in Equation (14). Finally, the calculation of *bnet* is shown in Equation (15).

$$Ah1 = 2D \cdot W + 2W \cdot (B - 2W) = 2W \cdot (D + B - 2W) \quad (11)$$

$$Ah2 = 2W \cdot (D - 2W) + 2W \cdot (B - 4W) = 2W \cdot (D + B - 6 \cdot W) \quad (12)$$

$$Ah\ total = Ah1 + Ah2 = 2W \cdot (D + B - 2W) + 2W \cdot (D + B - 6W) \quad (13)$$

$$Anet = bnet \cdot dnet = Atotal - Ah\ total = Atotal - [2W \cdot (D + B - 2W) + 2W \cdot (D + B - 6W)] \quad (14)$$

$$bnet = \frac{Atotal - [2W(D + B - 2W) + 2W(D + B - 6W)]}{dnet} \quad (15)$$

where, *dnet* is the net harvesting area length, m; *Ah total* is the area after the first and second round harvesting, m^2; *Anet* is net field area, m^2.

Now, the combine harvester has adequate area for harvesting and returns to the starting point. After that, the combine harvester travels straight to the headland and turns back. This Combine harvester's behavior loses time because the harvester has to lift its header and cannot harvest. This behavior is thus called the "headland turning lost time" (*Tnt*), shown in Equation (16). In addition, the amount of headland turning (*nnt*) is shown in Equation (17):

$$Tnt = ttn \cdot nnt \cdot knt \quad (16)$$

$$nnt = \left(\frac{bnet}{W}\right) - 1 \quad (17)$$

Combining Equations (16) and (17), the final *Tnt* becomes Equation (18) as follows:

$$Tnt = ttn \cdot knt \cdot \left\{ \frac{Atotal - [2W \cdot (D + B - 2W) + 2W \cdot (D + B - 6W)]}{d \cdot W} - 1 \right\} \quad (18)$$

where, *Tnt* is headland turning lost time, s; *ttn* is average headland turning lost time, s; *knt* is coefficient of the headland turning lost time; *nnt* is the amount of the headland turning, in a number of times.

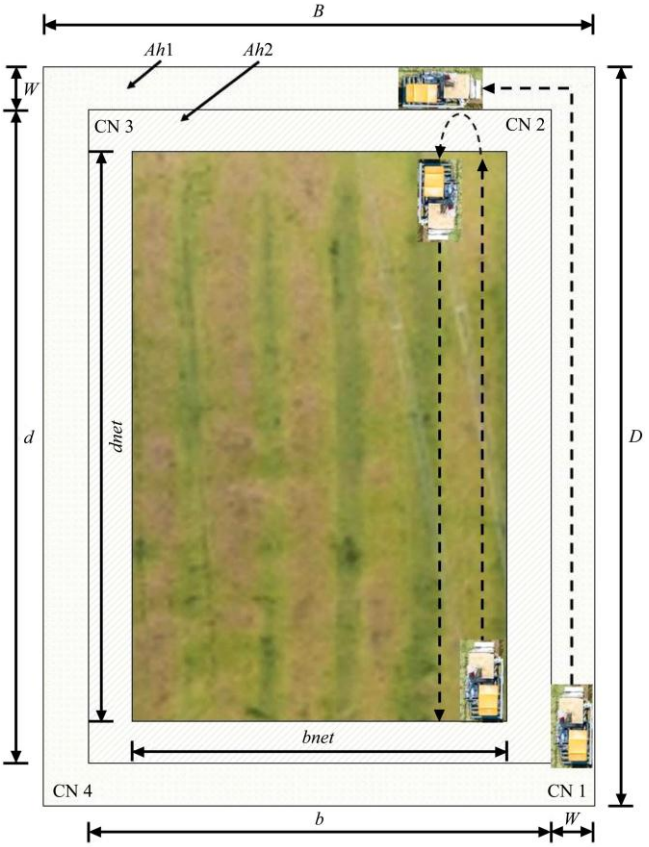

Figure 2 Dimensions and behavior of combine harvesters while harvesting in a practical field

2.3.3 Development of the prediction model for the travel and unloading of grain lost time (*Tf*)

Most rice combine harvesters have a grain tank for storing grain while harvesting in the field which is unloaded once the tank

is full, at which point a truck trailer comes to the field and travels next to the combine harvester. The combine harvester unloads the grain to the truck trailer and harvests continuously. On the other hand, the combine harvesters utilize a different process because the field conditions in Thailand and ASEAN differ from the United States and Europe, in that they have abundant mud and waterlogging. Furthermore, the truck trailer cannot come to the field and travel next to the Combine harvester. Thus, the combine harvesters have to spend additional time unloading. First, when the grain tank is full, the combine harvesters have to stop and travel to the truck trailer waiting on the road. This process is called the "traveling to unload lost time" (*Tfr*). Once the Combine harvester is in position for unloading, they will start to unload, which is called the "grain unloading lost time" (*Tfr*). The development of the prediction model for *Tfr* and *Tfs* is described in the following section.

2.3.3.1 Development prediction model for traveling to unload lost time (*Tfr*)

When combine harvesters have a full grain tank in the field they cannot continue to harvest and need to unload the grain first. The traveling distance is uncertain and depends on the volume of the grain tank. However, the approximate traveling distance can be calculated using the average distance between the field center and the unloading point (*Lavg*). First, the Tfr can be found by the ratio of all distances that exist between traveling from the field center to the truck trailer (*Ltotal*) and the traveling speed for unloading (*Sfr*), shown in Equation (19). However, the combine harvesters have to harvest all unharvested rice until the grain tank is full and then travel back to unload the grain once more in the practical harvesting. Furthermore, the amount of traveling to unload grain (*nfr*) is found by the ratio of the total yield of the field (*Ytotal*) and the grain tank volume (*ST*). Moreover, the *Ytotal* is found by multiplying the yield of a full grain tank (*Y*) and the *Atotal*; the *nfr* is shown in Equation (20). The combine harvesters have to harvest under varying conditions depending on crop, field and machine. Therefore, the coefficient of traveling to unload (*kfr*) was used to adjust the *Tfr* for accuracy. Finally, the *Tfr* can be found from Equation (21):

$$Tfr = \frac{Ltotal}{Sfr} = \frac{Lavg \cdot (2nfr - 1)}{Sfr} \tag{19}$$

$$nfr = \frac{Ytotal}{ST} = \frac{Y \cdot Atotal}{ST} \tag{20}$$

$$Tfr = \frac{kfr \cdot Lavg \cdot \left[\frac{2 \cdot (Y \cdot Atotal)}{ST} - 1 \right]}{Sfr} \tag{21}$$

where, *Tfr* is traveling to unload lost time, s; *Ltotal* is all distances between the field center to the truck-trailer, m; *Sfr* is traveling speed for unloading, m/s; *Lavg* is the average distance from the center of the field to the unloading point, m; *nfr* is the amount of time for traveling to unload, s; *Ytotal* is the total yield of the field, kg/m^2; *ST* is grain tank volume, kg; *Y* is the yield of a full grain tank, kg; *kfr* is coefficient of traveling to unload lost time.

2.3.3.2 Development of the prediction model for grain unloading lost time (*Tfs*)

When the Combine harvester has arrived at the unloading point, it adjusts itself to a suitable position before starting to unload. *Tfs* was calculated from the assumption that the combine harvester would unload when the grain tank is full. The *Tfs* can be found by the ratio of the *Ytotal* and the grain unloading rate (*R*) as shown in Equation (22):

$$Tfs = \frac{Ytotal}{R} \tag{22}$$

where, *Tfs* is grain unloading lost time, s; *R* is grain unloading rate, kg/s.

2.3.4 Development of the prediction model for repair, adjustment and refueling lost time during harvest (*Tm*)

During harvesting, the Combine harvester may encounter problems caused by defects such as broken belts or other accessories. Sometimes harvesters must stop for repairs, adjustments, or refueling[30,50]. Even though such problems do not occur too often, they result in extensive lost time. There are many factors affecting the Tm, such as rice varieties, field conditions, machine conditions and driver's experience. The *Tm* can be found by Equation (23):

$$Tm = \sum_{i=1}^{n} Tmn \tag{23}$$

where, $\sum_{i=1}^{n} Tmn$ is the total of repair, adjustment, and refueling lost time during the harvesting, s.

2.3.5 Development of the prediction model for bunds crossings lost time (*Tb*)

The *Atotal* is separated by three bunds into four small fields (Figure 3). Almost all drivers of this study prefer to finish their harvesting field by field, then cross the bund to the other fields. Thus the total bunds crossing time (*Cb*) is calculated using Equation (24). However, the combined harvesters encounter other factors affecting the bunds crossing, such as bund height, bund strength, the total weight of combine harvester and driver's experience in practical harvesting. Therefore, the coefficient of the bunds crossing lost time (*kb*) is used to adjust the *Tb* for accuracy as shown in Equation (25):

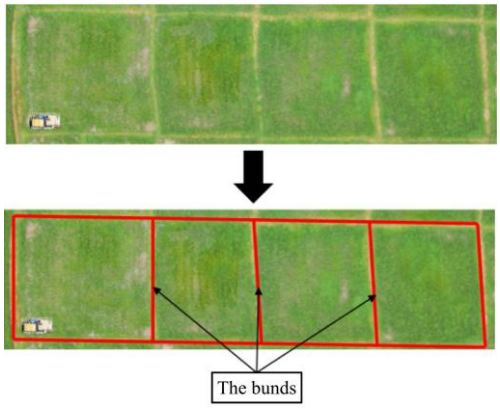

Figure 3 Aerial view of practical harvesting fields, separated into four smaller fields by the bunds

$$Cb = nb - 1 \tag{24}$$

$$Tb = kb \cdot Cb = kb \cdot (nb - 1) \tag{25}$$

where, *Cb* is total bunds crossing time, s; *nb* is number of small fields; *kb* is coefficient of the bunds crossing lost time

2.3.6 Fundamental prediction model of effective field capacity for Thai rice combine harvesters

By combining all prediction models of *Tth*, *Tn*, *Tf*, *Tm* and Tb the fundamental prediction model of effective field capacity (*EFC*) for Thai rice combine harvesters is shown in Equation (26):

$$EFC=\frac{Atotal}{\left(\frac{kth\cdot Atotal}{W\cdot S}\right)+\left\{tnt\cdot knt\cdot\left\{\frac{Atotal-[2W\cdot(D+B-2W)+2W\cdot(D+B-6W)]}{d\cdot W}-1\right\}\right\}+(\sum_{i=1}^{4}T1i+\sum_{i=1}^{4}T2i)}+\frac{Atotal}{\left\{\frac{kfr\cdot Lavg\cdot\left[\frac{2\cdot(Ytotal\cdot Atotal)}{ST}-1\right]}{Sfr}\right\}+\left(\frac{Y\cdot Atotal}{R}\right)+(\sum_{i=1}^{n}Tmn)+[kb\cdot(nb-1)]} \quad (26)$$

3 Methodologies

3.1 Development of the prediction model for effective field capacity

The fundamental prediction model for the *EFC* is shown in Equation (26). However, a difference in the physical properties of each rice variety might affect the effective field capacity of the Combine harvester. As such, the KDML-105 variety was selected in this study, which is the primary and most popular rice variety in Thailand for its high value and quality. This study began by collecting data such as field, crop and machine conditions from 15 randomly selected combine harvesters working in fields in November 2017. The time parameters (*Tth*, *Tnt*, *Tnc*, *Tfs*, *Tfr*, *Tm*, *Tb*) were collected by stopwatch. All data and time parameters will be used for calculating coefficients such as *kth*, *knt*, *kfr* and *kb*. Finally, the prediction model of effective field capacity for the KDML-105 variety ($EFC_{KDML\text{-}105}$) is shown in Equation (32).

3.2 Validation of the prediction model for the Thai hom mali rice variety

Validation of the aforementioned model should be repeated in order to confirm and assess the model. First, the data of the 12 combine harvesters working in the field in November 2017 were collected. The Root Mean Square Error (RMSE) is a technique used to measure the difference of effective field capacity between the prediction and the observational effective field capacity[51], as shown in Equation (27) below:

$$RMSE=\sqrt{\frac{\sum(EFC_{obs}-EFC_{prd})^2}{n}} \quad (27)$$

where, *RMSE* is the root mean square error; EFC_{obs} is observed effective field capacity, m^2/s; EFC_{prd} is predicted effective field capacity, m^2/s; *n* is the total number of combine harvesters.

The R^2 as shows the proportion of the variance in the independent variable that can be explained by the variance in the observed data, as shown in Equation (28)

$$R^2=1-\frac{\sum(EFC_{obs}-EFC_{prd})^2}{\sum(EFC_{obs}-\overline{EFC}_{obs})^2} \quad (28)$$

where, $\overline{EFC}_{obs}$ is mean of measured value (observe data).

The bias, which is the mean difference between the observed data and predicted data by effective field capacity model, which describes the overall accuracy of the calibration equation, as shown in Equation (29)

$$bias=\frac{\sum(EFC_{obs}-EFC_{prd})^2}{n} \quad (29)$$

4 Results

4.1 Development of the fundamental prediction model of effective field capacity

Equation (26) presents the fundamental prediction model of the *EFC* contained by the theoretical field time (*Tth*) and the total lost time during harvesting (*TL*). Additionally, the *TL* was calculated by the turning time on the headlands or corners of the field (*Tnt* and *Tnc*), the traveling for unloading and grain unloading time without harvesting (*Tfs* and *Tfr*), the repair, adjustment, and refueling time during the harvesting (*Tm*) and the bunds crossing lost time (*Tb*). First, the *Tth* includes parameters of *Atotal*, *W*, *S* and *kth*. Second, the *Tn* was calculated using *tnt*, *knt*, *Atotal*, *W*, *D*, *d*, $\sum_{i=1}^{4}T1i$ and $\sum_{i=1}^{4}T2i$. Third, the *Tf* was determined from *kfr*, *Lavg*, *Ytotal*, *Atotal*, *ST*, *Y* and *R*. Tm is the sum of repair, adjustment, and refueling time when the combine is required to stop during harvesting. Finally, the *Tb* consists of *kb* and *nb*. The coefficients (*kth*, *knt*, *kfr* and *kb*) were used to refine the fundamental prediction model and can be changed when predicting other rice varieties, as is true for *Tnc*, *Tm* and *R*.

4.2 Development of the prediction model of effective field capacity for the Thai hom mali rice variety

Table 1 shows the data of field, crop and machine conditions collected from the 15 combine harvesters. The averages of the field parameters (*Atotal*, *B*, *D*, *d*, *Lavg* and *nb*) are 8727.19 m^2, 45.69 m, 192.74 m, 186.35 m, 96.37 m and 1.47, respectively. Moreover, the averages of machine parameters (*W*, *ST*, *S*, *tnt* and *R*) are 3.19 m, 2420.00 kg, 1.73 m/s, 11.28 s and 10.46 kg/s, respectively, and the average crop parameter (*Y*) is 0.40 kg/m^2. The coefficient of the *Tth* (*kth*) was found using Equation (30) and calculated with the average *Atotal*, *W*, *S*, *Tth*. Second, the coefficient of the *Tnt* (*knt*), found in Equation (31), was calculated using the average *Tnt*, *Atotal*, *W*, *D*, *B*, *d*, *tnt* and *nnt*. Next, the coefficient of the *Tnt* (*kfr*) in Equation (32) was calculated using the average *Lavg*, *Tfr*, *Y*, *Atotal* and *ST*. Last, the coefficient of *Tb* (*kb*), found in Equation (33), was calculated using the average *nb* and *Tb*. The coefficients of *kth*, *knt*, *kfr* and *kb* were 1.72, 3.85, 0.96 and 72.94, respectively. Finally, the averages of *Tnc*, *Tm* and *R* were 148.42 s, 258.24 s and 10.46 kg/s, respectively. Furthermore, Table 2 shows the observed data of the 15 combine harvesters. The collected theoretical field time (*Tth*) and lost times during harvesting (*Tnt*, *Tnc*, *Tfs*, *Tfr*, *Tm* and *Tb*) show that the average *Tth* was 2645.51 s and the averages of *Tnt*, *Tnc*, *Tfs*, *Tfr*, *Tm* and *Tb* were 401.80 s, 148.42 s, 394.67 s, 306.95 s, 258.24 s and 34.04 s, respectively. In conclusion, the prediction model of effective field capacity to combine harvesters when harvesting the KDML-105 variety is shown in Equation (34).

$$kth=\frac{Tth\cdot W\cdot S}{Atotal} \quad (30)$$

$$knt=\frac{Tnt}{tnt\cdot\left\{\frac{Atotal-[2W\cdot(D+B-2W)+2W\cdot(D+B-6W)]}{d\cdot W}-1\right\}} \quad (31)$$

$$kfr=\frac{Tfr\cdot Sfr}{Lavg\cdot\left[\frac{2\cdot(Y\cdot Atotal)}{ST}-1\right]} \quad (32)$$

$$kb=\frac{Tb}{nb-1} \quad (33)$$

$$EFC_{KDML-105} = \frac{Atotal}{\frac{1.72 \cdot Atotal}{W \cdot S} + (3.85 \cdot tnt) \cdot \left\{ \frac{Atotal - [2 \cdot W(D+B-2 \cdot W) + 2 \cdot W(D+B-6 \cdot W)]}{d \cdot W} - 1 \right\} + 148.42} + \frac{Atotal}{\frac{0.96 \cdot Lavg \cdot \left(\frac{2 \cdot Y \cdot Atotal}{ST} - 1 \right)}{Sfr} + \frac{Y \cdot Atotal}{10.46} + 258.24 + 72.94 \cdot (nb-1)} \quad (34)$$

where, $EFC_{KDML\text{-}105}$ is a prediction model of effective field capacity for Combine harvester when harvesting the KDML-105 variety, m^2/s.

Table 1 Observed data of field, crop and machine conditions for the development of the fundamental prediction model

No.	Field						Machine							Crop
	Atotal/m^2	*B*/m	*D*/m	*d*/m	*Lavg*/m	*nb*/field(s)	*W*/m	*ST*/kg	*S*/m s^{-1}	*tnt*/s	*nnt*/times	*R*/kg s^{-1}	*Sfr*/m s^{-1}	*Y*/kg s^{-1}
P1	9948.07	38.71	260.35	253.71	130.18	1.00	3.32	2500.0	2.09	27.60	6.30	9.49	197.00	0.20
P2	5858.50	29.15	194.50	187.86	97.25	1.00	3.32	2500.00	1.96	11.58	3.91	12.63	542.00	0.24
P3	12157.24	36.99	171.51	165.43	85.76	1.00	3.04	2300.0	1.37	16.23	18.43	8.52	461.00	0.19
P4	16081.82	52.89	317.32	310.88	158.66	1.00	3.22	2500.0	0.90	17.68	10.47	5.10	91.00	0.32
P5	8305.78	74.89	110.99	104.71	55.50	1.00	3.14	2000.0	1.50	8.90	17.64	10.93	212.00	0.25
P6	1912.42	28.54	71.50	65.22	35.75	1.00	3.14	2000.0	1.50	8.00	2.97	11.84	61.80	0.25
P7	5331.97	66.72	90.93	84.65	45.46	2.00	3.14	2000.0	1.50	8.47	12.20	15.15	297.00	0.25
P8	6379.31	53.65	125.12	118.60	62.56	1.00	3.26	2500.0	2.23	5.67	9.91	8.04	148.00	0.47
P9	8877.49	53.38	164.44	157.92	82.22	1.00	3.26	2500.0	1.70	6.19	11.06	8.09	112.00	0.44
P10	11093.63	54.61	212.98	206.46	106.49	2.00	3.26	2500.0	2.43	6.74	10.55	11.20	166.00	0.44
P11	5796.55	20.54	297.70	291.18	148.85	2.00	3.26	2500.0	2.46	7.13	0.91	10.68	165.00	0.78
P12	13548.77	48.35	263.53	257.01	131.77	2.00	3.26	2500.0	2.05	8.89	10.52	9.27	183.00	0.78
P13	11374.57	41.81	311.67	305.57	155.84	4.00	3.05	2500.0	1.23	14.94	6.74	4.36	1588.00	0.27
P14	11666.09	51.42	222.18	216.18	111.09	1.00	3.00	3000.0	1.72	10.21	12.15	15.63	379.00	0.63
P15	2575.58	33.75	76.33	69.87	38.16	1.00	3.23	2500.0	1.24	11.00	4.85	16.03	63.00	0.50
Avg	8727.19	45.69	192.74	186.35	96.37	1.47	3.19	2420.0	1.73	11.28	9.24	10.46	311.05	0.40

Coefficient

kth	*knt*	*kfr*	*kb*
1.72	3.85	0.96	72.94

Table 2 Observed operating times for the development of the fundamental prediction model

No.	*Tth*/s	*Tn*		*Tf*		*Tm*/s	*Tb*/s
		Tnt/s	*Tnc*/s	*Tfs*/s	*Tfr*/s		
P1	1864.20	276.0	109.00	280.00	196.80	0.00	0.00
P2	2041.20	614.0	109.00	198.00	541.80	0.00	0.00
P3	3050.00	779.0	197.00	357.00	460.80	226.20	0.00
P4	5560.80	601.0	146.00	864.00	91.20	1752.00	0.00
P5	2544.20	347.0	72.00	367.00	211.80	0.00	0.00
P6	748.00	112.0	79.00	0.00	0.00	0.00	0.00
P7	3151.20	576.0	120.00	132.00	297.00	291.00	64.80
P8	1192.60	136.0	63.00	423.00	148.20	64.20	0.00
P9	2420.80	161.0	107.00	503.00	112.20	0.00	0.00
P10	2033.02	283.0	147.00	670.98	166.20	0.00	82.80
P11	1296.20	57.0	158.33	384.00	165.00	106.80	69.00
P12	3227.40	391.0	213.00	819.00	183.00	28.80	52.80
P13	5848.80	1255.0	435.00	574.00	1588.00	1203.00	241.20
P14	3976.00	296.0	108.00	192.00	379.20	61.80	0.00
P15	728.20	143.0	163.00	156.00	63.00	139.80	0.00
Avg.	2645.51	401.8	148.42	394.67	306.95	258.24	34.04

4.3 Validation of the prediction model of effective field capacity for the Thai hom mali rice variety

Table 3 shows the data of field, crop and machine conditions from the 12 combine harvesters in November 2017, and Table 4 shows the observed operating times. The observed effective field capacities of the 12 combine harvesters (EFC_{obs}) were calculated using Equation (3) and the results are shown in Table 4. The EFC_{obs} ranged from 1.37 m^2/s to 2.30 m^2/s. Furthermore, the parameters in Tables 3 and 4 were inserted into Equation (34) and used to predict the EFC_{obs} as shown in Table 5. The EFC_{prd} ranged

from 1.33 m^2/s to 2.36 m^2/s. Finally, the EFC_{prd} and the EFC_{obs} were validated with an *RMSE* of 0.24 m^2/s, an R^2 of 0.63 and *bias* 0.01 m^2/s as presented in Table 6 and Figure 4.

Table 3 Observed data of field, crop and machine conditions for validation of the prediction model

No.	Field						Machine							Crop
	Atotal/m^2	*B*/m	*D*/m	*d*/m	*Lavg*/m	*nb*/field(s)	*W*/m	*ST*/kg	*S*/m s^{-1}	*tnt*/s	*nnt*/times	*R*/kg s^{-1}	*Sfr*/m s^{-1}	*Y*/kg s^{-1}
V1	22191.55	81.14	279.36	272.72	139.68	2.0	3.32	2500.0	1.96	15.63	18.42	10.46	0.27	0.24
V2	2190.22	34.04	65.58	59.30	32.79	1.0	3.14	2000.0	1.50	9.06	4.89	10.46	2.28	0.25
V3	4309.91	55.80	85.09	78.81	42.55	1.0	3.14	2000.0	1.50	9.49	9.90	10.46	0.20	0.25
V4	7737.23	55.88	141.73	135.21	70.87	1.0	3.26	2500.0	2.06	7.96	11.09	10.46	0.52	0.44
V5	5165.28	49.71	99.42	92.90	49.71	1.0	3.26	2500.0	2.32	6.87	10.20	10.46	0.24	0.44
V6	8839.24	61.33	148.22	141.70	74.11	1.0	3.26	2500.0	2.57	6.69	12.59	10.46	0.16	0.56
V7	4659.93	49.33	96.45	89.93	48.23	1.0	3.26	2500.0	2.23	5.97	8.99	10.46	0.51	0.47
V8	12718.13	44.27	256.42	250.28	128.21	2.0	3.07	2500.0	1.44	10.63	10.94	10.46	0.68	0.42
V9	5040.77	47.77	126.34	120.20	63.17	1.0	3.07	2500.0	1.44	14.50	7.27	10.46	0.67	0.59
V10	2293.94	31.81	83.56	77.42	41.78	1.0	3.07	2500.0	1.44	16.52	3.32	10.46	3.87	0.59
V11	2436.1	33.17	71.96	65.50	35.98	1.0	3.23	2500.0	1.24	10.75	4.88	10.46	2.40	0.50
V12	6757.57	47.63	143.00	136.84	71.50	1.0	3.08	2200.0	1.14	14.58	9.82	10.46	0.38	0.56

Table 4 Observed operating times for validation of the prediction model

No.	*Tth*/s	*Tn*		*Tf*		*Tm*/s	*Tb*/s	EFC_{obs} /m^2 s^{-1}
		Tnt/s	*Tnc*/s	*Tfr*/s	*Tfs*/s			
V1	7113.38	625.0	287.0	514.8	613.02	1127.82	21.0	2.15
V2	1018.00	154.0	75.0	0.0	0.0	0.00	0.0	1.76
V3	1708.00	389.0	79.0	216.0	212.0	428.00	0.0	1.42
V4	2208.00	223.0	91.0	135.0	283.0	418.00	0.0	2.30
V5	1246.00	158.0	85.0	210.0	316.0	526.00	0.0	2.03
V6	1787.20	214.0	62.0	457.8	588.0	1045.80	0.0	2.13
V7	1246.80	209.0	62.0	94.2	298.0	392.20	0.0	2.02
V8	4188.00	457.0	166.0	189.0	487.0	676.00	46.2	2.05
V9	2022.20	348.0	85.0	94.8	232.0	326.80	0.0	1.62
V10	954.20	413.0	85.0	0.0	0.0	0.00	0.0	1.58
V11	1033.20	129.0	165.0	0.0	0.0	0.00	0.0	1.84
V12	3482.80	379.0	96.0	190.2	295.0	485.20	0.0	1.37

Table 5 Predicted operating times for validation of the prediction model

No.	*Tth*/s	*Tn*		*Tf*		*Tm*/s	*Tb*/s	EFC_{obs} /m^2 s^{-1}
		Tnt/s	*Tnc*/s	*Tfr*/s	*Tfs*/s			
V1	5865.75	1,109.09	148.42	1,617.11	511.31	258.27	72.94	2.32
V2	802.33	170.72	148.42	3.43	52.33	258.27	0.00	1.53
V3	1578.83	362.13	148.42	16.03	102.98	258.27	0.00	1.75
V4	1982.27	340.52	148.42	220.84	323.53	258.27	0.00	2.36
V5	1176.78	269.95	148.42	162.48	215.98	258.27	0.00	2.31
V6	1818.00	324.46	148.42	1,305.59	475.21	258.27	0.00	2.04
V7	1105.70	206.93	148.42	68.94	210.76	258.27	0.00	2.33
V8	4965.06	448.26	148.42	586.38	506.48	258.27	72.94	1.82
V9	1967.88	406.54	148.42	123.74	282.29	258.27	0.00	1.58
V10	895.54	211.68	148.42	0.78	128.46	258.27	0.00	1.40
V11	1045.18	202.33	148.42	3.55	116.42	258.27	0.00	1.37
V12	3325.39	551.77	148.42	447.32	363.30	258.27	0.00	1.33

Table 6 Root mean square error (RMSE) of the observed and predicted effective

No.	EFC_{obs}/m^2 s^{-1}	EFC_{prd}/m^2 s^{-1}	EFCobs-EFCprd	R^2	*RMSE*/m^2 s^{-1}	*Bias*/m^2 s^{-1}
V1	2.15	2.32	-0.17	0.63	0.24	0.01
V2	1.76	1.53	0.23			
V3	1.42	1.75	-0.33			
V4	2.3	2.36	-0.06			
V5	2.03	2.31	-0.28			
V6	2.13	2.04	0.09			

V7	2.02	2.33	-0.31
V8	2.05	1.82	0.23
V9	1.62	1.58	0.04
V10	1.58	1.4	0.18
V11	1.84	1.37	0.47
V12	1.37	1.33	0.04

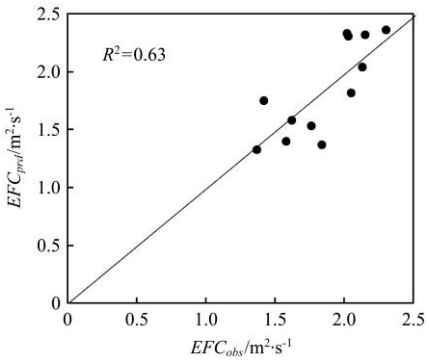

Figure 4 Relationship of the observed and predicted effective

5 Discussion

Equation (26) presents the coefficients (*kth*, *knt*, *kfr* and *kb*) used to refine the prediction model and their effect on *EFC*. This study used the KDML-105 rice variety as sample variety, and since the coefficients for each variety differ, other varieties should be studied for further research. The KDML-105 variety normally has a specific physical property, such as long stems and grains that easily fall from the ear. These specific physical properties affected the Tm of combine harvesters. Most combine harvesters would have to stop harvesting because the long stem of KDML-105 would jam the header unit. The driver experience affected the *Tnc* because the drivers' decisions affected the turning at the land corners. Meusel et al.[52] had evaluated the combine harvester operators with a combine simulator and the results found that the behavior of drivers influenced the lost times and effective field capacity. Not only driver experience but also field area affected the *Tnc*. Amiama et al.[27] studied the influence of field areas on lost times and concluded that there was a correlation between lost times and field areas. Furthermore, *R* is also influenced by the age of combine harvesters because most of the combine harvesters have been used for a long time, causing a decrease in combine harvester performance[53].

Figure 5 shows the percentage of *Tth* and total lost times (*TL*). The 12-validated combine harvester spent 64% and 36% of its time for the *Tth* and *TL*, respectively. However, the effective field capacity of combine harvesters decreased because of the effect of the *TL*. The *TL* was combined by 6 lost times (*Tnt*, *Tnc*, *Tfs*, *Tfr*, *Tm* and *Tb*) and Figure 6 shows the analysis of each lost time percentage. The *TL* can be separated into two groups, namely the major effect lost times and the minor effect lost times. The *Tm*, *Tfs* and *Tnt* constitute the major effect group and greatly impacted the effective field capacity, since each contributed 34%, 23% and 21% to the lost time, respectively. These lost times were influenced by the experiences of drivers and the age of combine harvesters[52]. On the other hand, the percentage of the minor effect group was *Tnc*, *Tfr* and *Tb* and these had 8%, 13% and 1% of lost time, respectively. These lost times were influenced by the field areas and yield, but they did not have a strong impact on the effective field capacity[27]. Finally, further research should be focused on how to decrease the lost times such as *Tm*, *Tfs* and *Tnt*. Furthermore, the model performance for other rice varieties should be studied as well.

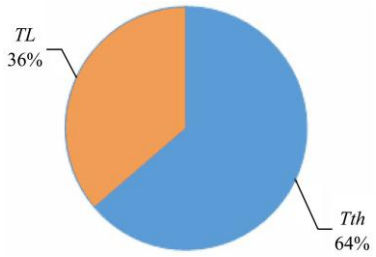

Figure 5 Operating times analysis of the 12-combine harvesters that were used for the development and validation of the prediction model

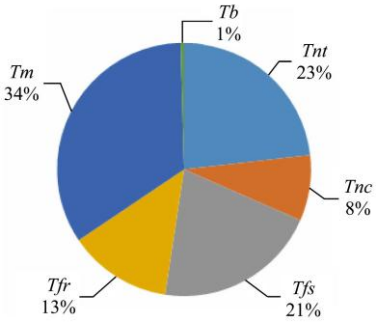

Figure 6 Analysis of the percentages of lost times of the 12-combine harvesters

6 Conclusions

The effective field capacity prediction model was validated using 15 combine harvesters, and then validated using 12 combine harvester to ensure predicting accuracy. Finally, the results show the root mean square error (*RMSE*) between the observed and predicted effective field capacity; the RMSE was 0.24 m^2/s. The RMSE is nearly zero, meaning that the mean the prediction model for the KDML-105 variety can be applied for estimating field capacity. The model could be used for selecting proper combine harvesters with their field condition, reducing harvest times, and achieving production capacity. However, other rice varieties should be studied for further research since the difference in physical properties in rice can cause effective field capacity change.

Acknowledgements

The authors express their gratitude and great appreciation to the Applied Engineering for Important Crops of the North-East Research Group; the Scholarship for Graduated Students of the Faculty of Engineering, Khon Kaen University; the Scholarship in Research for Dissertations of Graduated Students of the Faculty of Engineering; and, finally, Khon Kaen University for providing financial support for this research.

[References]

[1] Petley D. Global patterns of loss of life from landslides. Geology, 2012; 40: 927–930.
[2] Asseng S, Jamieson P D, Kimball B, Pinter P, Sayre K, Bowden J W, et al. Simulated wheat growth affected by rising temperature: increased water deficit and elevated atmospheric CO_2. Field Crops Research, 2004; 85(2): 85–102.
[3] Son N T, Chen C F, Chen C R, Chang L Y. Satellite-based investigation of flood-affected rice cultivation areas in Chao Phraya River Delta, Thailand. ISPRS Journal of Photogrammetry and Remote Sensing, 2013; 86: 77–88.
[4] The Mekong River Commission. Preparing the greater Mekong subregion flood and drought risk management and mitigation project. Laos: Mekong River Commission, Vientiane, 2008.
[5] FAO. Rice Market Monitor. Rome: Italy, 2011.
[6] Hirano T, Bekhasut P, Sommut W, Zungsontiporn S, Kondo A, Saka H, et al. Differences in elongation growth between floating and deepwater rice plants grown under severe flooding in Thailand. Field Crops Research, 2014; 160: 73–76.
[7] World-Bank.The world bank supports Thailand's post-floods recovery effort. 2011. http://www.worldbank.org/en/news/feature/2011/12/13/ world-banksupports-thailands-post-floods-recovery-effort. Accessed on [2018-01-12].
[8] OAE. Agricultural Statistics of Thailand. Thailand: Office of Agricultural Economics, 2011.
[9] Komori D, Nakamura S, Kiguchi M, Nishijima A, Yamazaki D, Suzuki S, et al. Characteristics of the 2011 Chao Phraya River flood in Central Thailand. Hydrological Research Letters, 2012; 6: 41–46.
[10] Buddhaboon C, Jintrawet A, Hoogenboom G. Effects of planting date and variety on flooded rice production in the deepwater area of Thailand. Field Crops Research, 2011; 124: 270–277.
[11] Fu J, Chen Z, Han L J, Ren L Q. Review of grain threshing theory and technology. Int J Agric & Biol Eng, 2018; 11(3): 12–20.
[12] He P, Li J, Zhang D, Wan S. Optimisation of the harvesting time of rice in moist and non-moist dispersed fields, Biosystems Engineering, 2018; 170: 12–23.
[13] Ebrahimi-Nik M A, Khademolhosseini N, Abbaspour-Fard M H, Mahdinia A, Alami-Saied K. Optimum utilisation of low-capacity combine harvesters in high-yielding wheat farms using multi-criteria decision making. Biosystems Engineering, 2009; 103(3): 382–388.
[14] Kalsirisilp R, Singh G. Adoption of a stripper header for a Thai-made rice combine harvester. Journal of Agricultural Engineering Research, 2001; 80(2): 163–172.
[15] Kleinhenz V, Chea S, Hun N. Survey of rice cropping systems in Kampong Chhnang Province, Cambodia. Rice Science, 2013; 20(2): 154–164.
[16] Baruah D C, Panesar B S. Energy requirement model for a combine harvester, Part I: Development of component models. Biosystems Engineering, 2005; 90(1): 9–25.
[17] Baruah D C, Panesar B S. Energy requirement model for combine harvester, Part II: Integration of component models. Biosystems Engineering, 2005; 90(2): 161–171.
[18] Jarolmasjed S, Abdollahpour S H, Gundoshmian T M, Ghazvini M A. Mathematical modeling of combine harvester header loss using dimensional analysis. EFITA-WCCA-CIGR Conference "Sustainable Agriculture through ICT Innovation". Turin, Italy, 24-27 June, 2013.
[19] Junsiri C, Chinsuwan W. Prediction equations for header losses of combine harvesters when harvesting Thai Hom Mali rice. Songklanakarin Journal of Science and Technology, 2009; 31(6): 613–620.
[20] Chuan-Udom S, Chinsuwan W. Threshing unit losses prediction for Thai axial flow rice combine harvester. Agricultural Mechanization in Asia Africa and Latin America, 2009; 40(1): 50–54.
[21] Sangwijit P, Chinsuwan W. Prediction equations for losses from Thai axial flow rice combine harvesters. Thai Journal of Agricultural Science, 2011; 44(1): 23–31.
[22] Liang Z, Li Y, Xu L, Zhao Z, Tang Z. Optimum design of an array structure for the grain loss sensor to upgrade its resolution for harvesting rice in a combine harvester. Biosystems Engineering, 2017; 157: 24–34.
[23] Siska J, Hurburgh Jr C R. Prediction of Wisconsin tester breakage susceptibility of corn from bulk density and NIRS measurements of composition. Transactions of the ASAE, 1994; 37(5): 1577–1582.
[24] Maertens K, De Baerdemaeker J, Ramon H, De Keyser R. An analytical grain flow model for a combine harvester, Part II: Analysis and application of the model. Journal of Agricultural Engineering Research, 2001; 79(2): 187–193.
[25] Maertens K, De Baerdemaeker J. Flow rate based prediction of threshing process in combine harvesters. Applied Engineering in Agriculture, 2003; 19(4): 383–388.
[26] Miu P I, Kutzbach H D. Mathematical model of material kinematics in an axial threshing unit. Computers and Electronics in Agriculture, 2007; 58: 93–99.
[27] Amiama C, Bueno J, Álvarez C J. Influence of the physical parameters of fields and of crop yield on the effective field capacity of a self-propelled forage harvester. Biosystems Engineering, 2008; 100(2): 198–205.
[28] Hirai Y, Inoue E, Mori K, Hashiguchi K. Power and machinery: investigation of mechanical interaction between a combine harvester reel

and crop stalks. Biosystems Engineering, 2002; 83(3): 307–317.

[29] Gundoshmian T M, Ghassemzadeh H R, Abdollahpour S, Navid H. Application of artificial neural network in prediction of the combine harvester performance. Journal of Food Agriculture and Environment, 2010; 8(2): 721–724.

[30] Doungpueng K, Chuan-Udom S. Effects of guide vane inclination patterns on threshing losses and power requirement. Kasetsart Journal (Natural Science), 2014; 48(1): 313–322.

[31] Khir R, Atungulu G, Ding C, Pan Z L. Influences of harvester and weather conditions on field loss and milling quality of rough rice. Int J Agric & Biol Eng, 2017; 10(4): 216–223.

[32] Hayashi S, Shigematsu K, Yamamoto S, Kobayashi K, Kohno Y, Kamata J, et al. Evaluation of a strawberry-harvesting robot in a field test. Biosystems Engineering, 2010; 105: 160–171.

[33] Van Henten E J, Van Tuijl B A J, Hemming J, Kornet J G, Bontsema J, Van Os E A. Field test of an autonomous cucumber picking robot. Biosystems Engineering, 2003; 86(3): 305–313.

[34] Zhao D, Lv J, Ji W, Zhang Y, Chen Y. Design and control of an apple harvesting robot. Biosystems Engineering, 2011; 110: 112–122.

[35] Si Y, Liu G, Feng J. Location of apples in trees using stereoscopic vision. Computers and Electronics in Agriculture, 2015; 112: 68–74.

[36] Bac C W, Hemming J, van Henten E J. Stem localization of sweet-pepper plants using the support wire as a visual cue. Computers and Electronics in Agriculture, 2014; 105: 111–120.

[37] Mehta S S, Burks T F. Vision-based control of robotic manipulator for citrus harvesting. Computers and Electronics in Agriculture, 2014; 102: 146–158.

[38] Zou X, Ye M, Luo C, Xiong J, Luo L, Wang H, et al. Fault-tolerant design of a limited universal fruit-picking end-effector based on vision positioning error. Applied Engineering in Agriculture, 2016; 32(1): 5–18.

[39] Wang C, Zou X, Tang Y, Luo L, Feng W. Localisation of litchi in an unstructured environment using binocular stereo vision. Biosystems Engineering, 2016; 145: 39–51.

[40] Gonzalez X P, Marey M F, Alvarez C J. Evaluation of productive rural land patterns with joint regard to the size, shape and dispersion of plots. Agricultural Systems, 2007; 92(1): 52–62.

[41] Kalsirisilp R, Singh G. Performance evaluation of a Thai-made rice combine harvester. Agricultural Mechanization in Asia Africa and Latin America, 1999; 30(4): 63–69.

[42] Win K M, Korinsak S, Jantaboon J, Siangliw M, Lanceras-Siangliw J, Sirithunya P, et al. Breeding the Thai jasmine rice variety KDML105 for non-age-related broad-spectrum resistance to bacterial blight disease based on combined marker-assisted and phenotypic selection. Field Crops Research, 2012; 137: 186–194.

[43] Hunt D. Farm power and machinery management. IA: Iowa St. U. Press. Ames, 1995.

[44] Chuan-Udom S. Grain harvesting machines. Khon Kaen: Khon Kaen University Press, 2013.

[45] Taylor R K, Schrock M D, Staggenborg S A. Extracting machinery management information from GPS data. Proceedings of the 2002 ASAE Annual International Meeting, Chicago, Illinois, July 28-31, 2002.

[46] Palmer R, Wild D, Runtz K. Improving the efficiency of field operations. Biosystems Engineering, 2003; 84: 283–288.

[47] Witney B. Choosing and using farm machines. Edinburgh: Land Technology Ltd, 1995.

[48] International Rice Research Institute (IRRI). Steps to successful in rice production. Philippines: Metro Manila, 2015.

[49] ASAE. The society for engineering in agricultural, food, and biological systems. Agricultural Machinery Management in ASAE Standards 1998. MI, 1998.

[50] Sangwijit P, Chinsuwan W. Prediction Equations for Losses of Axial Flow Rice Combine Harvester when Harvesting Chainat 1 Rice Variety. KKU Researh Journal, 2010; 15: 496–504.

[51] Mostafa K M, Quazi K H, Ehsan H C. Development of a remote sensing-based rice yield forecasting model. Spanish Journal of Agricultural Research, 2016; 14: 1–11.

[52] Meusel C, Grimm C, Gilbert S B, Luecke, G R. An agricultural harvest knowledge survey to distinguish types of expertise. In: Proceedings of the Human Factors and Ergonomics Society Annual Meeting, 2016; 60(1): 2048–2052.

[53] Esgici R, Sessiz A, Bayhan Y. The relationship between the age of combine harvester and grain losses for paddy. Scientific Proceedings IV International Scientific and Technical Conference Agricultural Machinery, 2016; pp.49–52.